Int. J. Electrochem. Sci., 6 **(2011)** 317 - 336

International Journal of ELECTROCHEMICAL SCIENCE
www.electrochemsci.org

Computational and Electrochemical Studies on the Redox Reaction of Dopamine in Aqueous Solution

H. Mohammad-Shiri[1], *M. Ghaemi*[2, *], *S. Riahi*[3, 4], *A. Akbari-Sehat*[3]

[1] Department of Chemistry, Tarbiat Modares University, P.O. Box: 14115-175, Tehran, Iran
[2] Department of Chemistry, Science Faculty, Golestan University, P.O. Box 49138-15739, Gorgan, Iran
[3] Center of Excellent in Electrochemistry, Faculty of chemistry, University of Tehran
[4] Institute of Petroleum Engineering, Faculty of Engineering, University of Tehran, P. O. Box 14399-57131, Tehran, Iran
[*]E-mail: ghaemi_m@gu.ac.ir

Received: 31 August 2010 / *Accepted:* 15 September 2010 / *Published:* 1 February 2011

The electrochemical behavior of dopamine, an important biological molecule, was investigated by means of cyclic voltammetry (CV) at various potential scan rates. All experiments were done in aqueous phosphate buffer solutions at different pHs. The experimental formal redox potential ($E^{o'}$) of dopamine was obtained to be 752 mV *versus* SHE (Standard Hydrogen Electrode). $E^{o'}$ values have also been calculated with the aid of density functional theory (DFT) method at B3LYP/6-311++G** basis set in conjunction with a Polarizable Continuum Model (PCM). Innovative application of both direct and indirect methods resulted in theoretical standard electrode potentials of the studied dopamine in the order of 782 and 710 mV, respectively. These results were found to be in excellent agreement with the experimental value in the order of 752 mV. Furthermore, Ultraviolet-visible (UV-vis) spectrum was evaluated by Time Dependent DFT (TD-DFT). Based on this study, characteristics of the electronic absorption spectrum in the visible and UV regions were assigned to π→π* transitions.

Keywords: Dopamine; Density functional theory; Cyclic voltammetry; Electronic structure

1. INTRODUCTION

Dopamine (3, 4-dihydroxyphenylethylamine, DAH_2), an important neurotransmitter, is existing in the mammalian central nervous system [1-3]. The oxidation of this catecholamine is interesting and this process occurs in the human body. Its improper regulation is associated with neurological diseases such as Parkinsonism, where dopamine levels are reduced and schizophrenia, which can be related to

excess activity of dopamine. Catecholamine drugs are also used to treat hypertension, bronchial asthma, organic heart disease and could be used in cardiac surgery and myocardial infarction [4].

Electrochemical behavior of dopamine plays important roles in its physiological functions, and is a key factor in diagnosis of some diseases in clinical medicine. Hence, it is desirable to develop an electrochemical method to study electron transfer processes [5-13]. The tendency of an organic species to donate or accept an electron in solution is measured by its (one-electron) standard redox potential (E^0). The measurement of this potential, which could be carried out for reversible reactions by cyclic voltammetry method, will be beneficial toward understanding and interpreting the mechanism of electron-transfer of innumerable physico-chemical and biological reactions. In the case of irreversible reactions or difficulty of experimental measurements, which may result from their associated complex chemical equilibria [14-20], useful models could be applied for prediction of these potentials [21].

The self-consistent reaction field (SCRF) theory [22-26] has been remarkably successful in describing the essential role of solvent effects on the molecule's geometry in solutions. In this work, SCRF theory and DFT methods were used for the molecular parameterization and calculation of electrode potentials of the studied compounds [27-31]. In this relation, we have studied the redox electrochemistry of dopamine (DAH_2) and its oxidized form (DA), (Scheme 1) both theoretically and experimentally. Furthermore, electronic absorption spectra, molecular geometry and vibrational frequencies of DAH_2 and DA were calculated using DFT for both gas phase and aqueous systems. The main aim of this study is to assess the accuracy of the quantum-chemical calculations of the redox potentials and structural properties of the studied compounds by comparing them with experimental data.

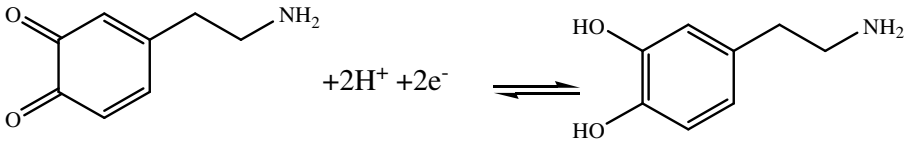

Scheme 1. The two protons, two-electron redox process of dopamine.

2. EXPERIMENTAL DETAILS AND CALCULATIONS

2.1. Materials and instruments

The electrochemical experiments were performed with the microAutolab potentiostat system III/FRA2 (EcoChemie B.V., The Netherlands), equipped with GPES 4.9 software. Dopamine (3,4-dihydroxyphenylethylamine), was of analytical grade and purchased from Sigma Aldrich. Phosphoric acid and its derivatives were obtained from Merck.

Cyclic voltammetry measurement was performed, using a three-electrode system in buffer solutions, at 25 ± 1 °C. The electrolyte, composed of a mixture of phosphoric acids and its derivatives,

was adjusted to the appropriate pH. The working electrode consisted of a pencil graphite electrode (PGE) (0.5 HB, Owner, made in Korea), which was insulated with Teflon, was then cut into a disk form. A platinum wire and Ag|AgCl||KCl (sat.) were used as the counter-and the reference electrodes, respectively.

2.2. Cyclic voltammetry of dopamine

In order to check the reversible behavior of dopamine redox reactions, cyclic voltammetry experiments were carried out between 0.2-0.7 V at various scan rates. As illustrated in Fig. 1, cyclic voltammograms of dopamine, at a fixed pH value of 2.1, shows enhancement of peak current with increasing scan rate. This implicates the especially fast electron transfer in dopamine without limiting behavior at high scan rates. As could be seen from Fig. 1, the ratio of peak current for both anodic and cathodic reactions is constant at different scan rates. At a scan rate of 25 (mV/s), the electrode gives a reversible voltammogram. We may assume that the rate of chemical reactions is not faster than the electron transfer under our experimental conditions. This assumption is based on the small molecular size of dopamine and the ortho positions of OH groups.

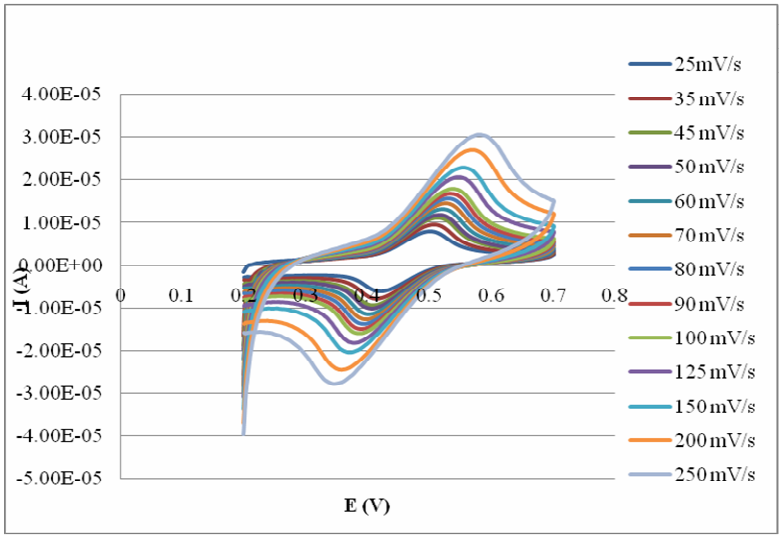

Figure 1. Effect of scan rates on the peak currents of dopamine (1×10^{-3} M) at pH= 2.1

The Peak-to-peak separation, between the corresponding anodic and cathodic peaks, increase with increasing scan rate, which points to quasi-reversible behavior. The reasons for much stronger pH-effect on increasing anodic and cathodic peak potential are two folds: on one hand, difficulty of releasing H^+ during oxidation of dopamine in acidic medium and on the other, increasing cathodic overpotential with increasing pH.

Fig. 2 shows the effects of pH on the positions of peak potentials. In the pH range of 2.1–3.4, anodic peaks have a little shift of about 8 mV, however, in the middle pH range of 3.4–5.1, a peak

potential position shift of about 52 mV was recorded. It could be assumed that in the middle pH range, the anodic overpotential is lower than that of acidic medium. The increasing trend in peak position shift of 115 mV could be observed in the pH range of 6.2–7.3 due to decreasing overpotential with increasing pH. Compared to anodic reaction, the reverse effect of pH on the peak potential was observed for cathodic region. In this region, for the first pH range of 2.1–3.4, the peak potential shift is about 60 mV and the slope of the curve is 66.3 mV/pH. This value implicates the separate transfer of electrons and protons due to lowest value of overpotential. In the middle pH range of 3.4–5.1, the peak potential shift of 84 mV is lower than the corresponding shift in the first acidic range in the order of 25 mV.

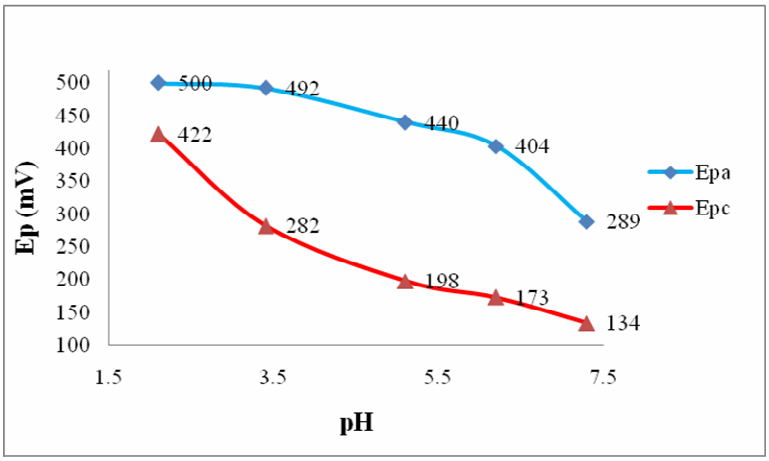

Figure 2. Effect of pH on peak potential positions at a fixed scan rate of 25 mV/s

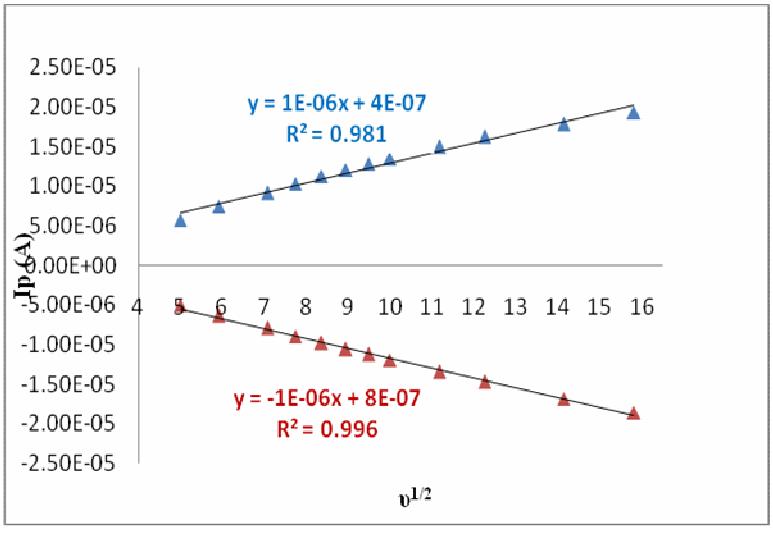

Figure 3. Anodic and cathodic peak current ratio for different sweep rates for dopamine at pH 2.1

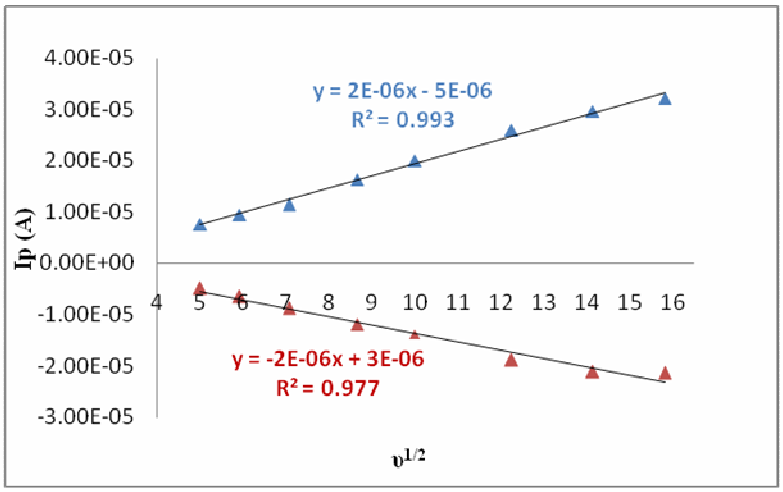

Figure 4. Anodic and cathodic peak current ratio for different sweep rates for dopamine at pH 7.3

The separation of cathodic and anodic peak potentials in the middle pH range indicated that the redox process of dopamine was quasi-reversible. Figs. 3 and 4 present the anodic and cathodic peak current ratio for different sweep rates at pH=2.1 and 7.3, respectively. As could be seen in both Figs. 3, 4, the relationship between peak current (I_p) and square root of scan rate ($\upsilon^{1/2}$) implicates that the IR Ohmic drop is negligible. This is due to similarity in the slopes of cathodic and anodic curves in the order of 1×10^{-6} and 2×10^{-6} for pH 2.1 and 7.3, respectively.

2.3. Calculation methods

The standard electrode potentials can be obtained theoretically by employing both indirect and direct methods

2.3.1. Indirect method

The general method for this kind of reaction is to calculate redox potentials of compounds which belong to one family, using an isodesmic reaction [32], by selecting one of them as a reference compound (here cathecol, CAH_2) according to the following reaction:

$$DA_{(sol)} + CAH_{2(sol)} \longrightarrow DAH_{2(sol)} + CA_{(sol)} \qquad \Delta G^{o}{}_{rxn} \tag{1}$$

Then, the standard electrode potential E^o of DAH_2 can be computed as:

$$E^{o} = E^{o}{}_{CAH_2} - \frac{\Delta G^{o}{}_{rxn}}{nF} \tag{2}$$

Where, $E°_{CAH2}$ is the experimental redox potential of CAH_2, n is the number of electrons transferred (in this case n=2) and F is the Faraday constant (96485.338 C mol^{-1}) [33, 34]. Furthermore, $\Delta G^{o}{}_{rxn}$, can be computed using the thermodynamic cycle depicted in Scheme 2. This could be written for the case of transferring all species involved in the reaction from the gas phase into the solution phase [35].

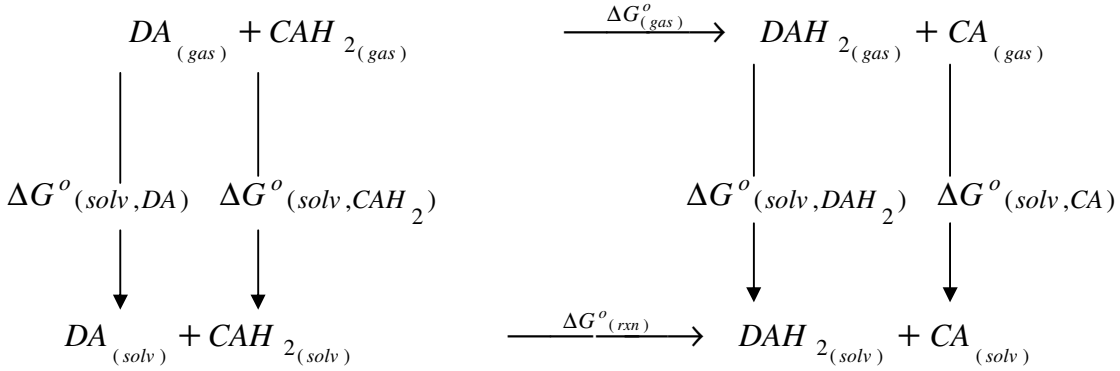

Scheme 2. The thermodynamic cycle used in calculation of $\Delta G^{o}{}_{rxn}$

In Scheme 2, $\Delta G°_{(g)}$ is the standard free energy of gas phase reaction (1) and $\Delta G^{o}{}_{(solv,i)}$ is the standard free energies of solvation of each component in water.

2.3.2. Direct method

The calculation of redox potential of a component, compared to SHE, is possible by calculation of Gibbs energy change of the following thermodynamic cycle (Scheme 3).

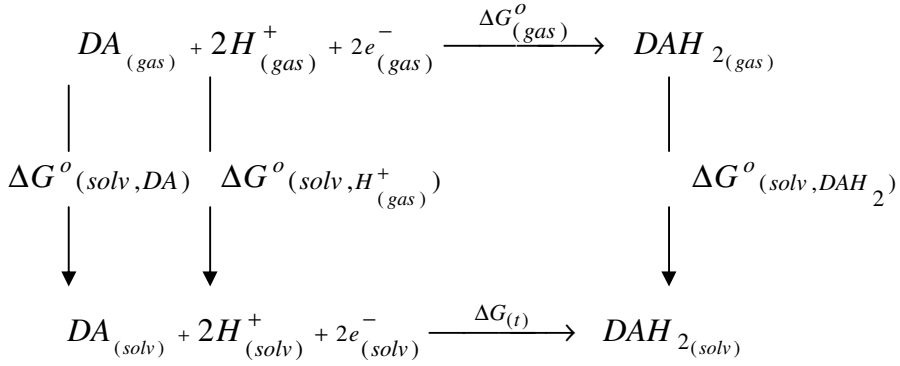

Scheme 3. Thermodynamic cycle designed to calculate $\Delta G_{(t)}$

The gas phase contribution to the Gibbs free energy can be determined using *DFT* calculations. These calculations have been performed at the DFT (B3LYP) level by using 6-31G* and 6-311++G** basis sets.

The theoretical G3 and CBS-Q methods indicated that accurate ionization potentials within negligible error resulted from this method of calculations although these methods are too demanding for general calculations. Ionization potential is defined as the enthalpy change of reaction 1 in the gas phase at 298.15 K and 1 atm. This potential, together with the standard redox potential, E^o, could be calculated using density functional theory (DFT). Other methods such as the HF and MP2 are known to be improper for such calculations [36].

The free energies of solvation of DA and DAH_2 at 298 K and 1 atm., were calculated using the polarized continuum (overlapping spheres) model (PCM) which developed by Tomasi and co-workers [37-39]. According to [39], the energy-minimized structure, created in the optimized step, was used as the basis for charge population calculations with a full natural bond orbital analysis (NBO) population method. All the calculations were performed using the DFT (B3LYP) and Gaussian03 suite of programs [41]. Electronic absorption were calculated using TD-DFT method at B3LYP/6-311++G** level. This may allow proper assignment of the excited-states and vertical excitation energy involved in the absorption process.

The imagining of atom movement was made feasible using the GaussView 4.4.2 [42]. The plot of theoretical spectrum and density of states (DOS) were drawn by GausssSum 0.8 package [43]. The experimental geometric data of the DAH_2 were taken from the crystallographic results dopamine.HCl [44].

3. RESULTS AND DISCUSSION

3.1. Geometry

Since the molecular parameters are controlled by the molecular geometry, the optimization of geometry is the most important step for the calculation of the formal potential. The optimized structures are true energy-minimums as no imaginary frequency is predicted. The geometries and serial number of atoms in both DAH_2 and DA are shown in Fig. 5. All atoms of the benzene ring in both DAH_2 and DA, which have a C_1 axis of symmetry, are about planar. Their bond lengths and bond angles were optimized at the B3LYP/6-31G*, 6-311++G** levels. Table 1 compares our calculated structural parameters of DAH_2 with those of X-ray crystallography data [44]. As could be seen from Table 1, the bond lengths and angles of the same molecules at DFT-B3LYP/6-311++G** level are in good agreement with those at DFT-B3LYP/6-31G* level as well as with experimental data. Correlations between calculated and experimental bond lengths are shown in Fig. 6.

The R (4, 5), R (1, 6) bond lengths decreased from 1.396 Å, 1.400 Å to 1.344 Å, 1.351 Å respectively. This could be due to transformation of aromatic bonding in DAH_2 into the double bonding in DA. Furthermore, due to the presence of two carbonyl groups in DA, the bond lengths of R (1, 2), R (2, 3) and R (3, 4) in DAH_2 are shorter than those in DA. As a result, the A(1,2,3), A(1,2,7),

A(2,3,4), A(2,3,8), A(4,5,6), A(5,6,1), A(5,6,9) bond angles should also change noticeably with changes of bond lengths.

The distribution of NBO charges at B3LYP/6-311++G** of title molecules in water shows that the natural charges of C2, C3 are more positive in DA than those of DAH_2 (Fig. 7). This could be attributed to a rather more electronegativy of SP^2 hybridization of O7, O8 in DA than that of the SP^3 hybridization of the corresponding atoms in DAH_2.

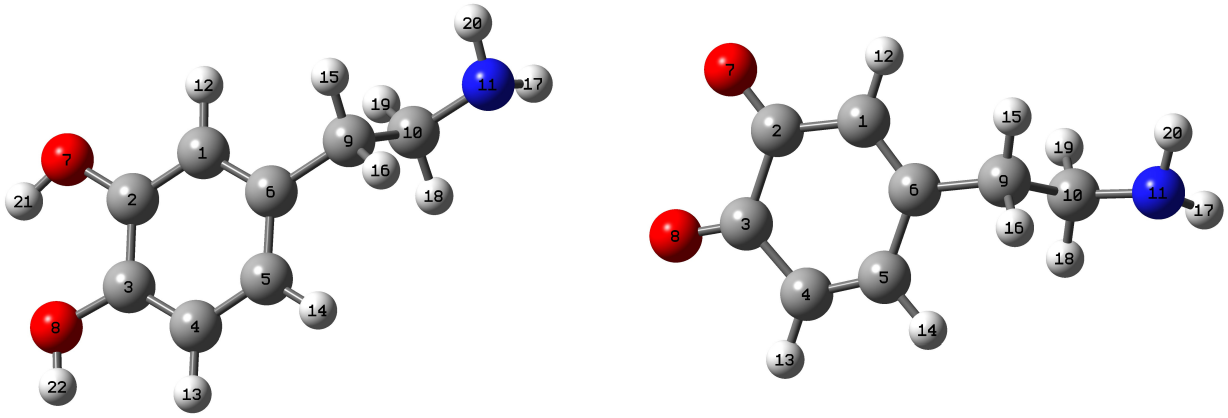

(a) (b)

Figure 5. Serial number of atoms and optimized geometries of DAH_2 (a) and DA (b) at B3LYP/6-311++G** level

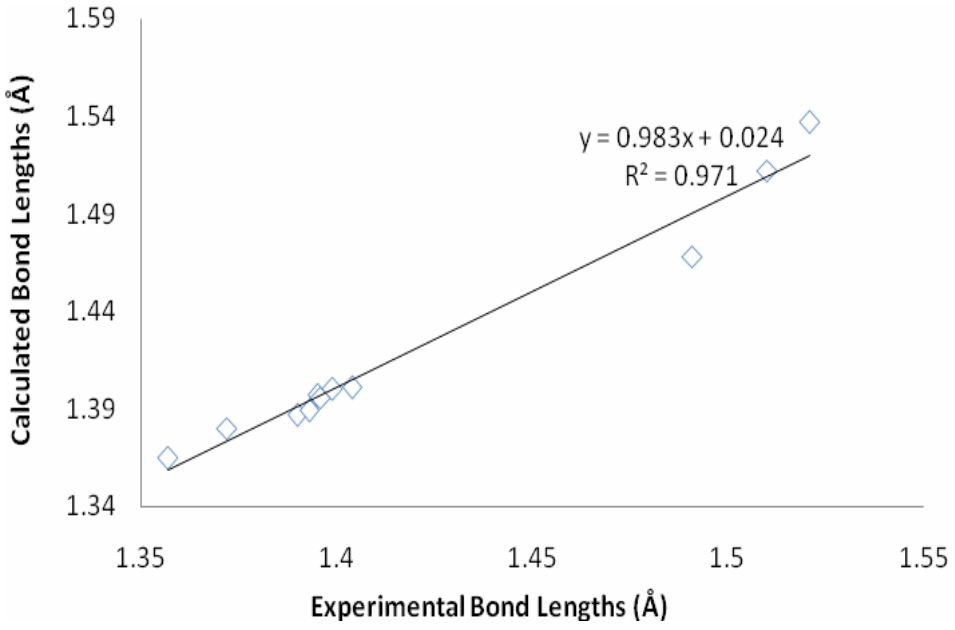

Figure 6. Calculated bond length in comparison with experimental data at B3LYP/6-311++G** level

Table 1. The geometry parameters of DAH_2 and DA

Compound	DAH_2		DA		DAH_2
Basis set	6-31G*	6-311++G**	6-31G*	6-311++G**	Exp[a]
Bond length (Å)					
R(1,6)	1.430	1.400	1.355	1.351	1.399
R(1,2)	1.391	1.389	1.469	1.468	1.393
R(2,3)	1.405	1.400	1.558	1.565	1.403
R(3,4)	1.389	1.387	1.474	1.473	1.389
R(4,5)	1.399	1.396	1.349	1.344	1.396
R(5,6)	1.399	1.397	1.473	1.473	1.395
R(2,7)	1.365	1.365	1.220	1.213	1.357
R(3,8)	1.380	1.380	1.218	1.211	1.372
R(6,9)	1.513	1.512	1.507	1.505	1.510
R(9,10)	1.538	1.537	1.542	1.541	1.521
R(10,11)	1.467	1.468	1.464	1.464	1.490
			Bond angle (deg)		
A(1,2,3)	119.5	119.6	117.2	117.1	119.91
A(1,2,7)	120.1	119.8	123.0	123.1	118.63
A(2,3,4)	120.1	120.0	116.8	116.6	119.78
A(2,3,8)	115.0	115.3	120.3	120.4	116.73
A(3,4,5)	119.9	120.0	120.6	120.6	119.93
A(4,5,6)	120.8	120.8	123.3	123.4	120.89
A(5,6,1)	118.6	120.9	120.1	120.3	118.87
A(6,9,10)	112.8	112.9	112.7	112.7	110.75
A(9,10,11)	110.3	110.4	109.8	110.0	110.84
A(5,6,9)	120.9	120.9	117.5	117.4	120.73
A(6,1,2)	121.1	121.1	121.9	121.1	120.6
			Dihedral angle (deg)		
D(6,1,2,3)	0.005	0.079	0.27	0.25	0.28
D(6,1,2,7)	-179.84	-179.82	-179.59	-179.63	-179.98
D(1,2,3,4)	0.071	0.080	0.13	0.27	0.66
D(1,2,3,8)	179.84	179.86	179.98	179.86	177.53
D(2,3,4,5)	-0.11	-0.11	-0.36	-0.51	-0.21
D(3,4,5,6)	-0.035	-0.021	-0.22	-0.26	-0.64
D(4,5,6,1)	0.083	0.18	0.19	0.28	1.01
D(4,5,6,9)	177.99	178.11	178.69	178.80	176.20
D(5,6,9,10)	93.44	94.55	73.48	73.80	100.47
D(6,9,10,11)	177.72	178.39	174.69	175.10	171.77
D(9,6,1,2)	177.95	178.09	178.39	178.51	176.67
D(7,2,3,8)	0.05	0.13	0.11	0.02	2.16
D(8,3,4,5)	179.86	179.87	179.75	179.62	177.85

a: These values were taken from [44].

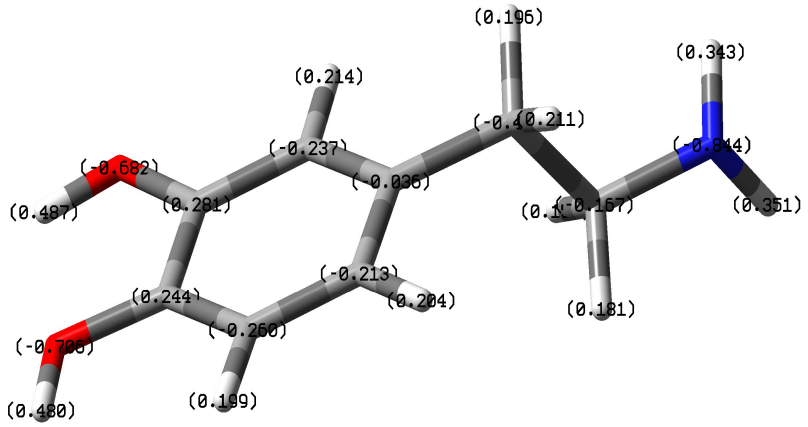

(a)

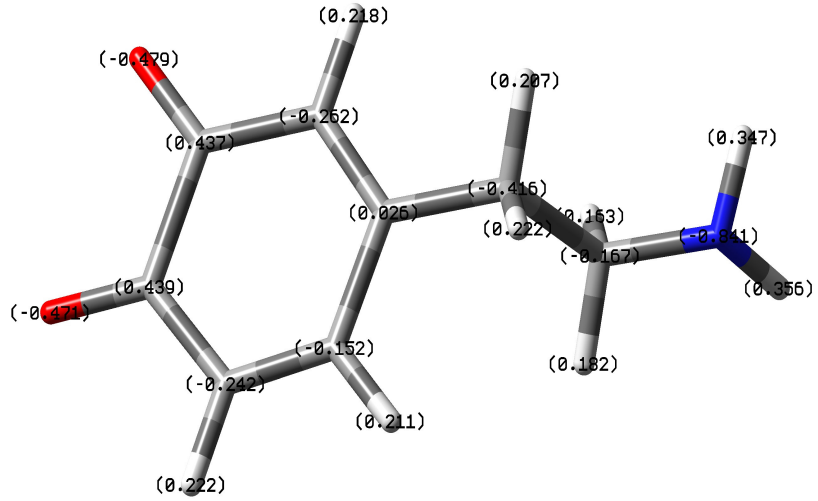

(b)

Figure 7. NBO charges distribution of (a) DAH_2 and (b) DA in water at B3LYP/6-311++G** level.

3.2. Electrochemical behavior and calculation of electrode potentials

Fig. 8 displays the dependence of the measured formal potential values of the DA/DAH_2 redox system on the pH values. The standard potential values (E^0) could be fitted by means of Eq.3. $E^{o'}$ value of the redox system DA/DAH_2, (Eq. 4), was obtained from the intercept of straight line presented in Fig. 8 and is equal to 558 mV *versus* Ag/AgCl (sat.), KCl (3M)**:**

$$E^o = -47.93pH + 558.4(mV) \qquad (R^2 = 0.997) \tag{3}$$

$$E = E^{o'} - 2.303(mRT/nF)pH \tag{4}$$

In Eq. 4, (m) and (n) are number of H^+ (protons) and electrons in the redox couple (here m=n=2), respectively, and all other symbols have their conventional meaning. The potential of Ag/AgCl electrode *versus* SHE is given as follows:

$$E_{Ag/AgCl(3M,KCl)} = E^0_{Ag/AgCl} - 0.059\log[Cl^-]$$
$$= 0.222V - 0.059\log 3 = 0.194V(1atm,\ \ 25^oC) \quad (5)$$

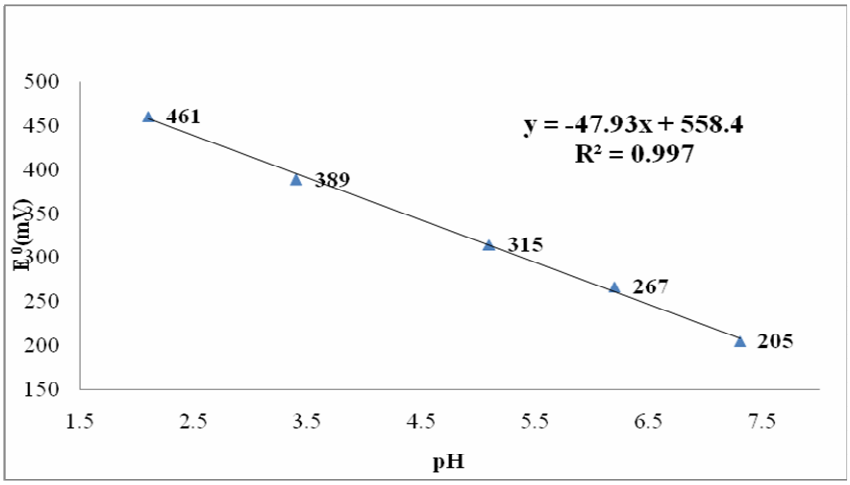

Figure 8. Plot of formal potentials *versus* pHs

Thus the standard reduction potential of DAH_2 is 752 mV *versus* SHE. From cycle showed in Scheme 2, ΔG^o_{rxn} is computed by the following expression:

$$\Delta G^o_{rxn} = \Delta G^o_{gas} + \Delta(\Delta G^0_{sol}) \quad (6)$$

where ΔG^o_{gas} is the standard Gibbs free energy of reaction (1) in the gas phase and $\Delta(\Delta G^0_{sol})$ is the net free energy of solvation of reaction (1) in water. Table 2 summarized the calculated Gibbs free energies of the molecules in their reduced and oxidized form in gas and solution phases by density functional theory (DFT) using frequency calculations. Furthermore, the free energies of solvation were computed in order to convert the gas-phase energies to the energies in the solution phase. Electrode potentials of DAH_2 and DA were accomplished with the aid of total Gibbs energies and the experimental electrode potential values of the reference molecule cathecol CAH_2 (as mentioned in section 2.3.1 and illustrated in Scheme 2). Table 3 presents the electrode potential of title molecule, calculated at the B3LYP/6-31G*, 6-311++G** level.

Table 2. The Gibbs free energy of the title molecule for both reduced (red.) and oxidized (ox.) forms in the gas- and solution phases, along with the change of Gibbs free energy of reaction (1), ΔG_1, in both gas and solution phases

Mol.[a]	$\Delta G^{b}_{(gas)}$		$\Delta G_{(sol)}{}^{b}$		ΔG^{b}_{1}	
	Red.	Ox.	Red.	Ox.	Gas	Solution
1[c]	-382.729561	-381.49346	-382.753368	-381.515729	0	0
2[c]	-516.679182	-515.448705	-516.709440	-515.475069	0.002738	0.003268
1[d]	-382.620808	-381.392240	-382.620908	-381.392233	0	0
2[d]	-516.507058	-515.291813	-516.53427	-515.314144	0.0013323	0.008549

a: 1: RED.=CAH_2, OX.= CA, 2: RED.= DAH_2, OX.= DA
b: These energies are in atomic units, Hartree (1 Hartree = 2625.49975 kJ mol^{-1})
c: These energies have been calculated at B3LYP level using 6-311++G** basis set
d: These energies have been calculated at B3LYP level using 6-31G* basis set

Table 3. Electrode potential of the studied molecules in water, compared with the experimental value.

Mol.[a]	E_{exp}(mV)[b, c]	$E^{o'}$ (mV)[d]	$E^{o'}$ (mV)[e, f]
1	792[b]	_	827[e]
2	752[c]	658	710[f]

[a]1=cathecol, 2=dopamine
[b]The experimental electrode potential of cathecol is taken from [45].
[c]The experimental electrode potential as explained in text.
[d]Electrode potential calculated by Eq. 2 as explained in the text in B3LYP level and 6-31G* basis set.
[e]Electrode potential calculated by direct method as explained in the text in B3LYP level and 6-311++G** basis set.
[f] Electrode potential calculated by Eq. 2 as explained in the text in B3LYP level and 6-311++G** basis set.

The redox standard potential calculated with the 6-311++G** basis set, which includes both polarization and diffuse functions, is in a better agreement with those of experimental.

In order to calculate redox potential of DAH_2, by using direct method on the basis of thermodynamic cycle (Scheme 3), $\Delta G^{*}(t)$ could be calculated using following equation:

$$\Delta G^{*}(t) = \Delta G^{o}_{gas}(1M) + \Delta(\Delta G^{*})(solv, DAH_2 - DA) - 2\Delta G^{*}(H^{+}, solv) \quad (7)$$

Differences between the reference states of the gas-phase (1 atm, 24.46 L at 298.15 K) and PCM solvation calculations (1M) were calculated *via*:

$$\Delta G^{o}_{gas}(1M) = \Delta G^{o}_{gas}(1atm) + \Delta nRTLn(24.46) \quad (8)$$

where $\Delta G^{o}_{gas}(1atm)$ is the change of Gibbs free-energy (Scheme 3), Δn (equal -2) is the net change of moles (Scheme 2), $\Delta(\Delta G^{*})(solv, DAH_2 - DA)$ is the net free energy of solvation of DAH_2 in water.

Based on Electron Convention on Fermi-Dirac statistics (EC-FD), the energy and entropy of free electrons were reported to be 3.720 kJ mol^{-1} and 22.734 J mol^{-1} K^{-1}at 298.15 K, respectively [46]. The Gibbs free energy of $H^{+}_{(gas)}$ has been reported to be -26.3 kJ mol^{-1} [47]. Calculation of the redox potential of DAH_2 in direct method also requires the experimental standard Gibbs free energy of solvation of H^{+} in water.

Unfortunately, the precise calculation of $\Delta G^{*}(H^{+}, solv)$ on the basis of SHE measurements is uncertain and ranges from -254 to -261 kcal.mol^{-1}. The Uncertainty is based on the fact that SHE could not be attainable by measurements alone [48-50]. In this case, an independent quantity is required to determine an absolute half-cell potential. Therefore, we have used a value of -261 kcal/mol (-1092.0 kJ mol^{-1}) for $\Delta G^{*}(H^{+}, solv)$ in aqueous solution.

On the basis of equation: E°= -ΔG*(t)/nF and using data in Table 4, the absolute redox potential of DA/DAH_2 has been calculated in the order of 5.22 V. By selection of the absolute value of redox potential of SHE in the order of 4.44 V [51], $E^{o'}$ has been calculated to be 0.782 V. The calculated redox potential for DAH_2 in indirect (at 6-311++G** level) and direct method were 710 and 782 mV, respectively. These results are in excellent agreement with the experimental results of cyclic voltammetry for DA/DAH_2 in the order of 752 mV.

Table 4. The results of DFT calculations of DAH_2 and DA, together with Gibbs free energies of solvation of species computed at B3LYP/6-311++G** level of theory

	DA	DAH_2	Scheme 1
$\Delta G°_{gas}$ [a]	-1353310.4	-1356541.1	-3165.8
ΔnRT Ln (24.46)[a]	7.9	7.9	-15.8
Δ ΔG*(solv)[a]	-69.2	-79.4	2173.8[b]
ΔG*(t)[a]	-1353371.7	-1356612.6	-1007.8

[a]These energies are as kJ mol-1

[b]The free energy of solvation of proton has been considered as -1092.0 kJ. mol^{-1} to be consistent with other components

3.3. Electronic absorption spectra and eigenvalues of LUMO and HOMO for DAH_2/DA

The energy values of lowest unoccupied molecular orbital (LUMO) and the highest occupied molecular orbital (HOMO) and their energy gaps reflect the chemical activity of molecules. LUMO as an electron acceptor represents the ability to obtain an electron, HOMO represents the ability to donate an electron. The data for DAH_2 and DA, calculated at B3LYP/6-31G*, 6-311++G** levels, are presented in Table 5.

Table 5. Calculated eigenvalues of HOMO and LUMO, together with their energy gap

Basis set	**6-31G***				**6-311++G****			
Species	DAH_2		DA		DAH_2		DA	
Phase state	gas	solution	gas	solution	gas	solution	gas	solution
E_{HOMO}(eV)	-5.47	-5.46	-6.68	-6.01	-5.93	-5.94	-7.14	-6.78
E_{LUMO}(eV)	0.21	0.25	-3.46	-3.41	-0.52	-0.37	-3.92	-3.85
E_{LUMO}-E_{HOMO}(eV)	5.68	5.71	3.22	2.60	5.41	5.27	3.22	2.93

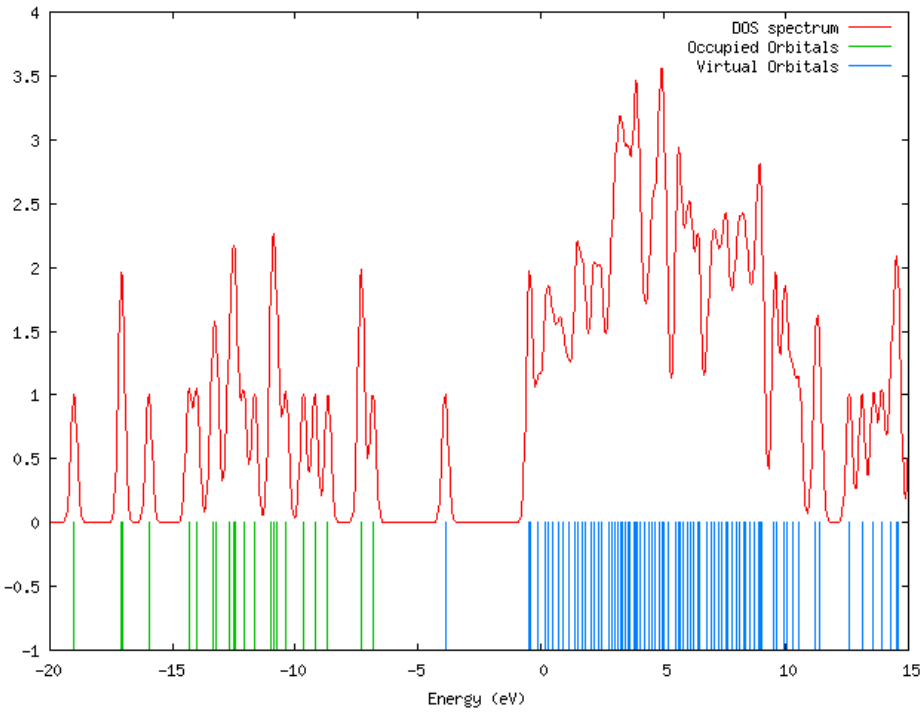

(a)

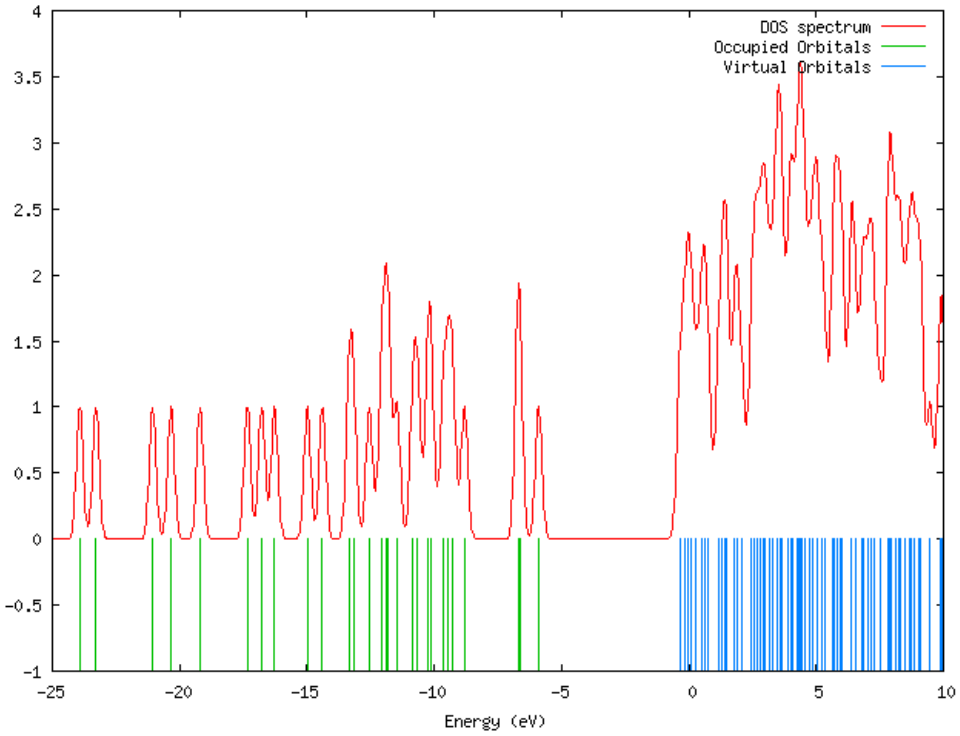

(b)

Figure 9. Frontier molecular orbital energies and corresponding density of states (DOS) spectrum of the (a) DAH_2 and (b) DA in water at B3LYP/6-311++G** level

Fig. 9 represents the frontier molecular orbital energies corresponding density of states (DOS) spectrum of DAH_2 and DA (in water) at B3LYP/6-311++G** level. Furthermore, the electronic densities in the HOMO and LUMO states of DAH_2 and DA in water are displayed in Fig. 10. These are mainly located on the benzene ring and hydroxyl groups, indicating that benzene ring and hydroxyl groups are active sites. Additionally, the data in Table 5 reveals that the energies of LUMO of DA are lower than those of DAH_2 and the energy gap of DA is smaller than that of DAH_2. Hence, transfer of electrons from HOMO to the LUMO in DA is easier than in DAH_2. Based on energies of HOMO and LUMO and the energy gaps of DA in both gas and water phases the energy of HOMO of DA increases. Furthermore the energy gap of HOMO and LUMO of DA in water is lower than that in the gas phase. Hence, it may be concluded that the activity of DA in water is higher than in the gas phase.

Table 6 shows the excitation energies (ΔE_{exc}) and oscillator strengths (f) of DAH_2 in the gas and water phases (PCM model), calculated at TD-DFT/6-311++G** level. From these data, UV/vis absorption spectra of DAH_2, in the range of 200-700 nm wavelengths, were simulated. This is adjusted by assigning to each transition a Gaussian function of which the height is proportional to the oscillator strength in both solvent and gas phases. Typical results are represented in Fig. 11. It may be remarked for DAH_2, that the absorption in the visible portion is much weaker than that in the UV portion. The

results of TD-DFT have a discernible red-shift in both gas and water phases; however, this shift is more significant in water phase compared to that in the gas phase.

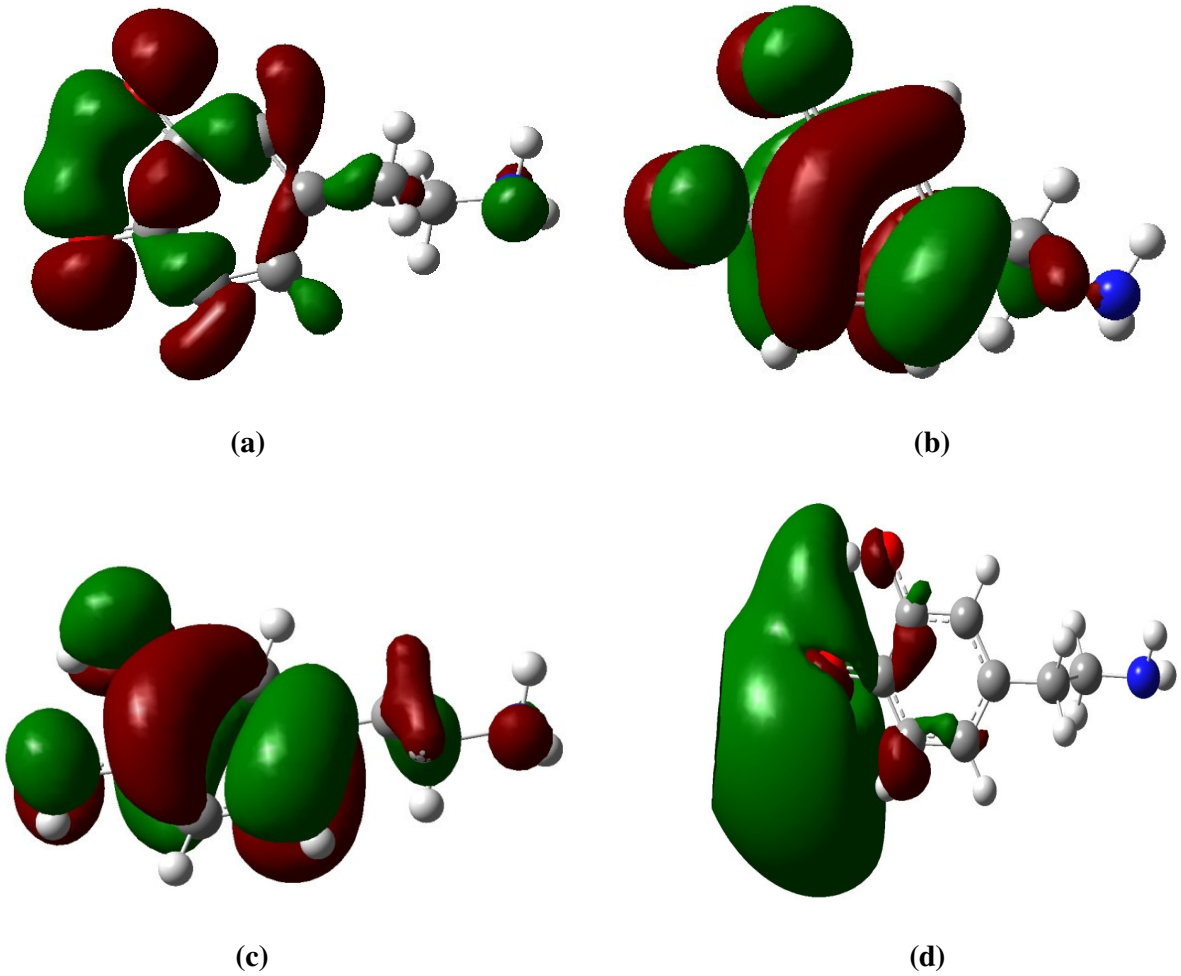

Figure 10. The electronic density in the HOMO and LUMO states of DAH_2 and DA computed by the B3LYP/6-311++G** method.(a) HOMO orbital for DAH_2; (b)LUMO orbital for DAH_2; (c) HOMO orbital for DA; (d) LUMO orbital for DA (isodensity value is 0.03 a.u).

The reason for differences between gas and solvent effects in TD-DFT calculations can be discussed from two points of view: First, the smaller gap of materials induces smaller excited energies. Second, reaction medium, in particularly polar solvents, could affect the geometry and then electronic structure. Table 6 shows the lowest excitation energies of DAH_2 in water in the order of 4.515 eV, which is close to the energy gap of the HOMO and the LUMO of DAH_2 in water (5.57 eV at 6-311++G** basis set). The HOMO-LUMO energy gap of DA in water at B3LYP/6-311++G** theory level is smaller than that in the gas phase. This fact shows that, unlike DAH_2, the solvent effects

stabilize the frontier orbitals of DA. Considering the instability of the latter, as an intermediate of the electrode process, its experimental spectra cannot be obtained.

Table 6. Excitation energies (ΔE_{exc}), and oscillator strengths (f) of dopamine calculated at TD-DFT/6-311++G** in the gas and water (PCM model)

State	ΔE_{exc}(eV)		f		Wavelength (nm)		λ_{max} [52]
	Gas phase	Water	Gas phase	Water	Gas phase	Water	
41→42	4.6041	4.5159	0.0009	0.0008	269	275	
39→45 40→45 41→43	4.8490	4.8280	0.0597	0.0584	256	257	281
39→44 40→44 41→44 41→47	5.1907	5.1642	0.0004	0.0004	239	240	
39→42 40→42 41→45 41→46 41→47	5.3412	5.2726	0.0012	0.0003	232	235	
39→42 40→42 40→44 41→45 41→46	5.4006	5.3325	0.0059	0.0028	230	233	
39→42 39→44 40→44 41→44 41→46 41→47	5.4427	5.4516	0.0143	0.00199	228	227	
39→43 39→44 40→43 41→45 41→46 41→47	5.5446	5.5225	0.0224	0.0194	224	225	220
40→43 41→44 41→46 41→47 41→48	5.6607	5.6212	0.0099	0.0032	219	221	
39→42 39→43 40→42 40→43 40→44 41→44 41→47 41→48	5.6799	5.7018	0.0038	0.0106	218	217	
39→42	5.7377	5.7275	0.0001	0.0016	216	216	
39→43 40→42 40→43							

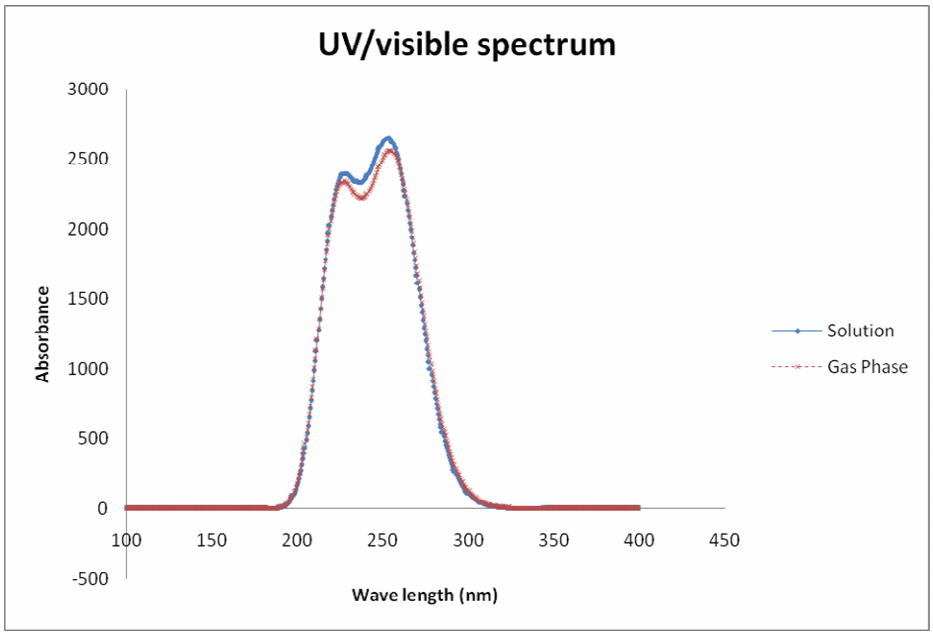

Figure 11. Simulated electronic absorption spectra of the DAH_2 in the (a) gas phase (b) solution phase.

Based on oscillator strengths and excitation energies (ΔE_{exc}), the peaks of DAH_2 in UV/vis spectrum appear at 281 and 220 nm [52]. These are in agreement with the calculating peaks found at 257 and 225 nm, respectively. These electronic transitions are directly related to those of the parent benzene molecule at 185, 202 and 254 nm. In benzene, the first band is assignable to a strong allowed $\pi \rightarrow \pi^*$ transition and the last two are the weak symmetry-forbidden transitions L_a and L_b. On the other hand substitutions on the benzene ring depend on the intensity of perturbation, lower symmetry and involve some allowed character into symmetry-forbidden transitions. By considering these factors, we could assign the transitions at 220 and 280 nm in DAH_2, with two hydroxyl and one aliphatic groups substituents, to a $\pi \rightarrow \pi^*$ and L_a - L_b coincident transitions, respectively.

4. CONCLUSIONS

1. Results obtained in this study show that the electrochemical behaviors of dopamine strongly depend on the pH values of the solutions. Electrode potential of the studied title molecule in aqueous solution can be theoretically calculated using DFT method, at the level of B3LYP and employing 6-311++G** basis set, as well as by cyclic voltammetry.
2. Theoretical and experimental results for standard electrode potentials of dopamine are in excellent agreement with each other as well as with the results of direct and indirect method, with a discrepancy in the order of 32-42 mV, respectively.
3. The geometries/electronic structures, HOMO and LUMO of dopamine were studied by using DFT with functional B3LYP and the UV-vis spectra were investigated *via* TD-DFT method. It

is found that solvent and energy gap compounds affect the electronic transitions and hence the shape of UV/vis spectra.

References

1. P. Damier, E. C. Hirsch, Y. Agid and A. M. Graybiel, *Brain*, 122 (1999) 1437
2. C. Martin, *Chem. Br.,* 34 (1998) 40
3. A. Heinz, H. Przuntek, G. Winterer and A. Pietzcker, *Nervenarzt,* 66 (1995) 662
4. J. R. Cooper, F. E. Bloom and R. H. Roth, *The Biochemical Basis of Neuropharmacology*; Oxford University Press, NewYork, 1986
5. R. N. Adams, *Anal. Chem.* 48 (1976) 1128A
6. S. H. Kim, J. W. Lee and I. H. Yeo, *Electrochim. Acta,* 45 (2000) 2889
7. H. M. Zhang, X. L. Zhou, R. T. Hui, N. Q. Li and D. P. Liu, *Talanta,* 56 (2002) 1081
8. H. Zhao, Y. Zhang and Z. Yuan, *Anal. Chim. Acta,* 441 (2002) 117
9. M. B. Gelbert and D. J. Curran, *Anal. Chem.,* 58 (1986) 1028
10. J. A. Stamford, *Anal. Chem.,* 58 (1986) 1033
11. T. F. Kang, G. L. Shen and R. Q. Yu, *Anal. Chim. Acta,* 354 (1997)343
12. Q. Wang, D. Dong and N. Li, *Bioelectrochemistry,* 54 (2001) 169
13. H. M. Zhang, N. Q. Li and Z. Zhu, *Microchem. J.,* 64 (2000) 277
14. F. Faridbod, M. R. Ganjali, R. Dinarvand, P. Norouzi and S. Riahi, *Sensors*, 8 (2008) 1645
15. F. Faridbod, M. R. Ganjali, B. Larijani, P. Norouzi, S. Riahi and F. Sadat Mirnaghi, *Sensors*, 7 (2007) 3119
16. S. Riahi, M. R. Ganjali, P. Norouzi and F. Jafari, *Sens. Actuators B*, 132 (2008) 13
17. C. A. Reynolds. *J. Am. Chem. Soc*., 112 (1990) 7545
18. C. A. Reynolds, W. G. Richards and P. J. Goodford. *J. Chem. Soc. Perkin Trans. II*., (1990) 551
19. C. A. Reynolds, P. M. King and W. G. Richards. *J. Chem. Soc. Chem. Commun*., (1988) 1434
20. P. Winget, E. J. Weber, C. J. Cramer and D. G. Truhlar. *Phys. Chem. Chem. Phys*., 2 (2000) 1231
21. J. B. Li, C. J. Cramer and D. G. Truhlar. *Biophys. Chem.*, 78 (1999) 147
22. M. Jalali-Heravi and M. Namazian, *J. Electroanal. Chem.,* 425 (1997)139
23. L. Onsager, *J. Am. Chem. Soc.,* 58 (1936) 1486
24. M. W. Wong, M. J. Frisch and K. B. Wiberg, *J. Am. Chem. Soc.,* 113(1991) 4776
25. M. Namazian, P. Norouzi and R. Ranjbar, *J. Mol. Struct. (Theochem),* 625 (2003) 235
26. M. Namazian, *J. Mol. Struct. (Theochem),* 664-665 (2003)273
27. Riahi S, Eynollahi S, Ganjali MR, Norouzi P, *Int. J. Electrochem. Sci.,* 5 (2010) 815
28. S. Riahi, S. Eynollahi, M.R. Ganjali, P. Norouzi, *Int. J. Electrochem. Sci.,* 5 (2010) 355
29. Riahi S, Mashhadi A, Eynollahi S, Ganjali MR, Norouzi P, *Int. J. Electrochem. Sci.,* 5 (2010) 955
30. Faridbod F, Ganjali MR, Nasli-Esfahani E, Riahi S, Norouzi P, *Int. J. Electrochem. Sci*., 5 (2010) 880
31. F. Faridbod, M.R. Ganjali, B. Larijani, E. Nasli-Esfahani, S. Riahi, P. Norouzi, *Int. J. Electrochem. Sci.,* 5 (2010) 653
32. M. W. Wong, K. B. Wiberg and M. J. Frisch, *J. Am. Chem. Soc*., 114 (1992) 1645
33. S.G. Lister, C.A. Reynolds and W.G. Richards, *Int. J. QuantumChem.,* 41 (1992) 293
34. M. Jalali-Heravi, M. Namazian and T. E. Peacock, *J. Electroanal.Chem.,* 385 (1995) 1
35. S. Riahi, S. Eynollahi, S. Soleimani, M. R. Ganjali, P. Norouzi and H. M. Shiri, *Int. J. Electrochem. Sci.,* 4 (2009) 1407
36. B. S. Jursic, *J. Mol. Struct. (THEOCHEM),* 452 (1998) 145
37. R. Bonaccorsi, R. Cimiraglia and J. Tomasi, *Comput. Chem.,* 4 (1983) 36
38. J. L. Pascualahuir, E. Silla, J. Tomasi and R. J. Bonaccorsi, *Comput. Chem.,* 8 (1987) 778
39. S. Miertus, E. Scrocco and J. Tomasi, *Chem. Phys.,* 55 (1981) 117

40. A. E. Reed, L. A. Curtiss, F. Weinhold, *Chem. Rev.,* 88 (1988) 899
41. M. J. Frisch, G. W. Trucks, H. B. Schlegel, G. E. Scuseria, M. A. Robb, J. R. Cheeseman, J. A. Montgomery, Jr., T. Vreven, K. N. Kudin, J. C. Burant, J. M. Millam, S. S. Iyengar, J. Tomasi, V. Barone, B. Mennucci, M. Cossi, G. Scalmani, N. Rega, G. A. Petersson, H. Nakatsuji, M. Hada, M. Ehara, K. Toyota, R. Fukuda, J. Hasegawa, M. Ishida, T. Nakajima, Y. Honda, O. Kitao, H. Nakai, M. Klene, X. Li, J. E. Knox, H. P. Hratchian, J. B. Cross, C. Adamo, J. Jaramillo, R. Gomperts, R. E. Stratmann,O. Yazyev, A. J. Austin, R. Cammi, C. Pomelli, J.W. Ochterski, P.Y. Ayala, K. Morokuma, G. A. Voth, P. Salvador, J. J. Dannenberg, V. G. Zakrzewski, S. Dapprich, A.D. Daniels, M. C. Strain, O. Farkas, D. K. Malick, A. D. Rabuck, K.Raghavachari, J. B. Foresman, J.V. Ortiz, Q. Cui, A. G. Baboul, S. Clifford, J. Cioslowski, B. B. Stefanov, G. Liu, A. Liashenko, P. Piskorz, I. Komaromi, R. L. Martin, D. J. Fox, T. Keith, M. A. Al-Laham, C. Y. Peng, A. Nanayakkara, M. Challacombe, P. M. W. Gill, B. Johnson, W. Chen, M. W. Wong, C. Gonzalez and J. A. Pople, *Gaussian 03*, Revision B.05; Gaussian, Inc.: Pittsburgh, PA, 2003
42. R. Dennington, T. Keith, J. Millam, *Gauss View 4.1*; Semichem, Inc.: Shawnee Mission, KS, 2007
43. N. M. O'Boyle and J. G. Vos, *Gauss Sum 0.8*, Dublin City University, 2004
44. C. L. Klein, *Struct. Chem.,* 2 (1991) 507
45. H. S. Rzepa and G. A. Suner, *J. Chem. Soc. Chem. Commun.,* (1993) 1743.
46. J. E. Bartmess, *J. Phys. Chem.,* 98 (1994) 6420
47. M. D. Liptak, K. G. Gross, P. G. Seybold, S. Feldgus and G. C. Shields, *J. Am. Chem. Soc.,* 124 (2002) 6421
48. C. Lim, D. Bashford and M. Karplus, *J. Phys. Chem., 95* (1991) 5610
49. H. Reiss and A. Heller, *J. Phys. Chem., 89* (1985) 4207
50. Y. Marcus, *Ion Solvation*; John Wiley and Sons: Ltd., 1985, pp.105-109
51. A. J. Bard and L. R. Faulkner, *Electrochemical Methods: Fundamentals and Applications*, Wiley, New York, 2001
52. W. J. Barreto, S. Ponzoni and P. Sassi, *Spectrochimica Acta Part A,* 55 (1999) 65